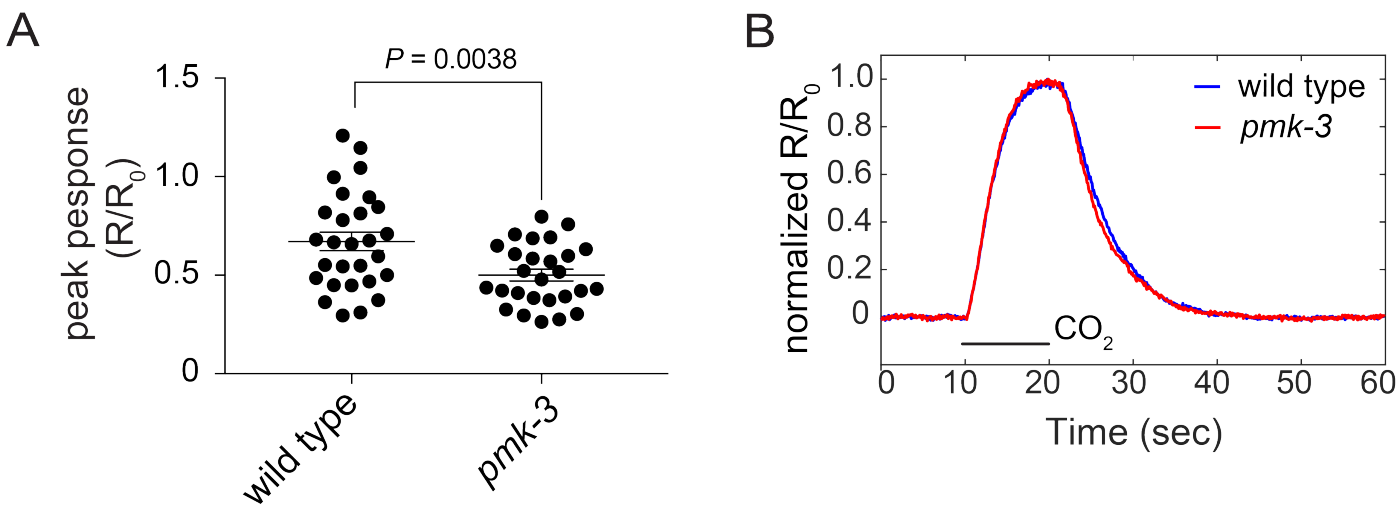

Figure S1: *pmk-3* mutant BAG neurons exhibit impaired chemotransduction in CO_2-sensing BAG neurons.

A. Scatter plots showing the distribution of peak calcium responses (R/R_0 values) of wild-type and *pmk-3(ok169)* mutant BAG neurons to 10% CO_2 stimuli. N > 26 animals/genotype. *P* = 0.0038, unpaired t-test. Error bars represent SEM.

B. The dynamics of the average calcium responses of wild-type and *pmk-3(ok169)* mutant BAG neurons to 10% CO_2 stimuli are indistinguishable.

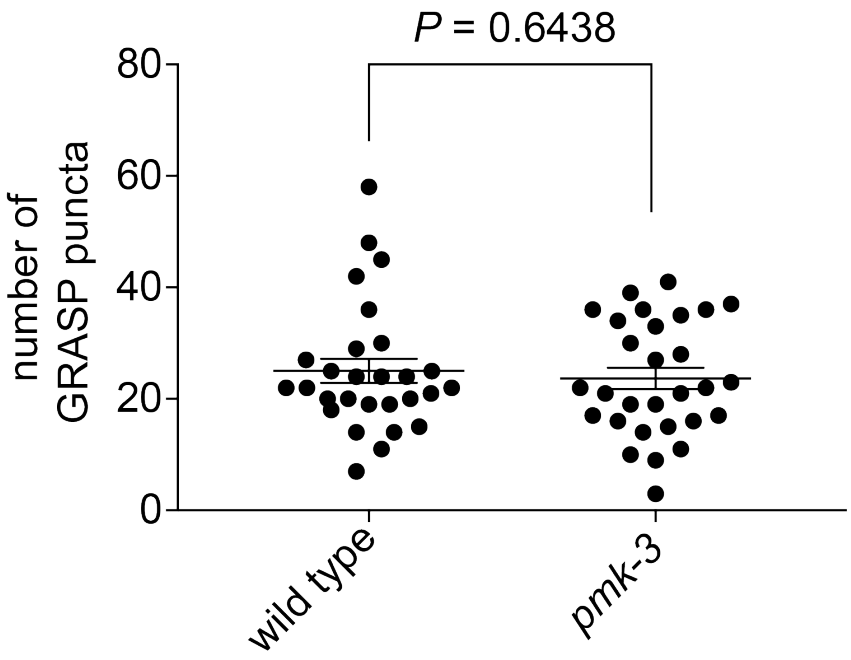

Figure S2: *pmk-3* mutant BAG neurons form normal number of synapses.

Scatter plot showing the number of GRASP-puncta in wild-type and *pmk-3(ok169)* mutant BAG neurons. *P* = 0.6438, unpaired t-test. N > 28 animals/genotype. Error bars represent SEM.

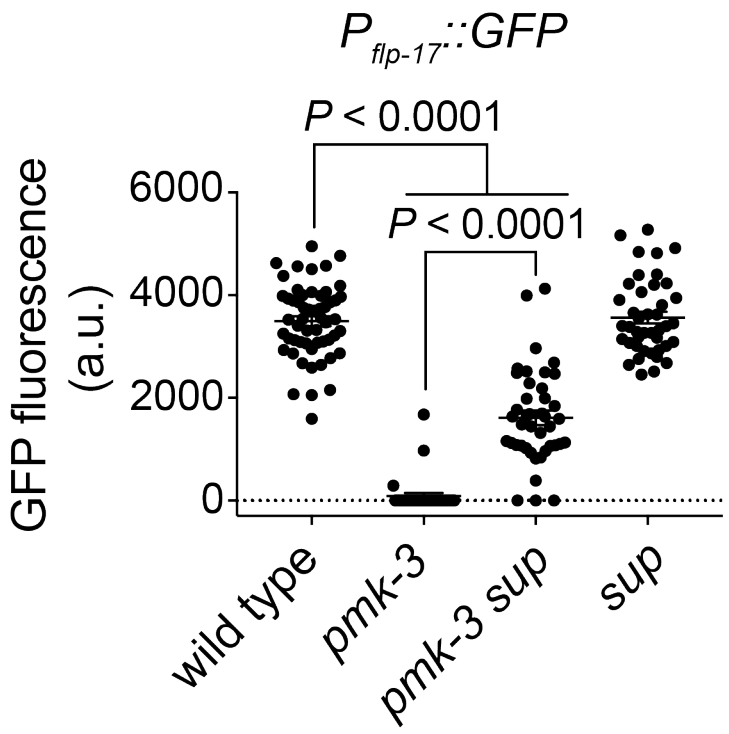

Figure S3: Suppressor mutations partially restore the levels of *flp-17* reporter expression to *pmk-3* mutant BAG cells.

Levels of P_{flp-17}*::GFP* expression in the wild-type, *pmk-3(wz31)*, *pmk-3(wz31) sup(wz75)*, and *sup(e169)* mutant animals. (****) $P < 0.0001$, ordinary one-way ANOVA followed by Tukey's multiple comparison test. N > 20 animals/genotype. (a.u.) arbitrary units. Bars represent mean ± SEM.

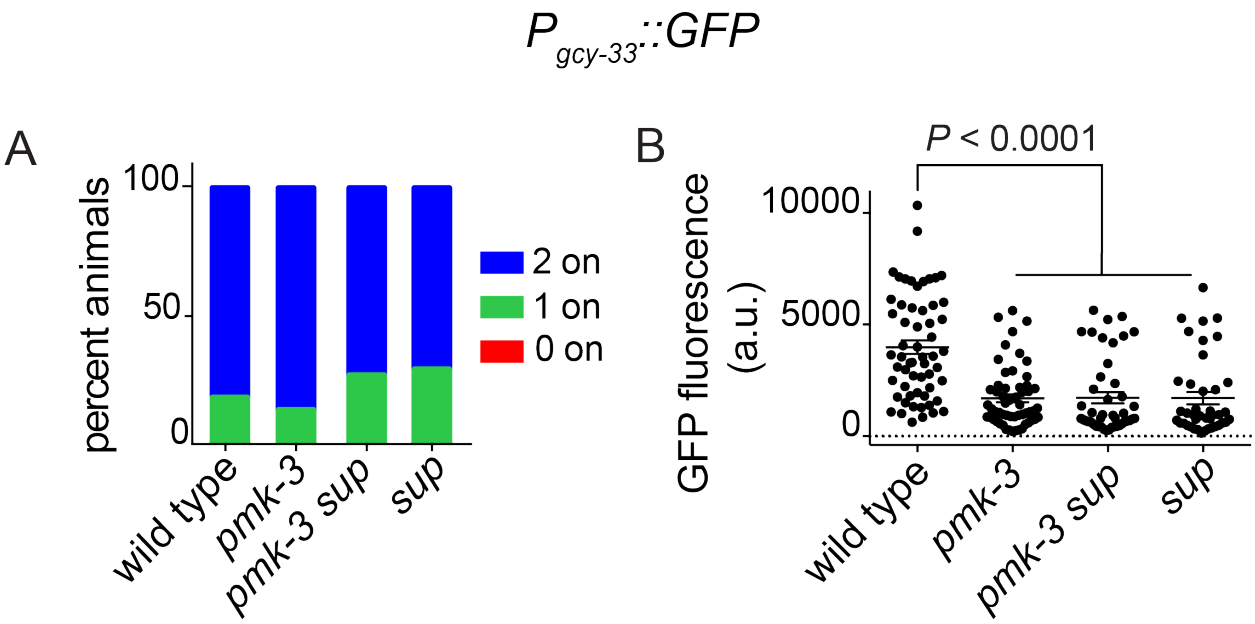

Figure S4: Suppressor regulates some, but not all, PMK-3 regulated genes in BAG neurons.

A. Penetrance of P_{gcy-33}*::GFP* expression in the wild-type, *pmk-3(wz31)*, *pmk-3(wz31) sup(wz75)*, and *sup(e169)* mutant animals.

B. Levels of P_{gcy-33}*::GFP* expression in the wild-type, *pmk-3(wz31)*, *pmk-3(wz31) sup(wz75)*, and *sup(e169)* mutant animals. (****) $P < 0.0001$, ordinary one-way ANOVA followed by Tukey's multiple comparison test. N > 20 animals/genotype. (a.u.) arbitrary units. Bars represent mean ± SEM.

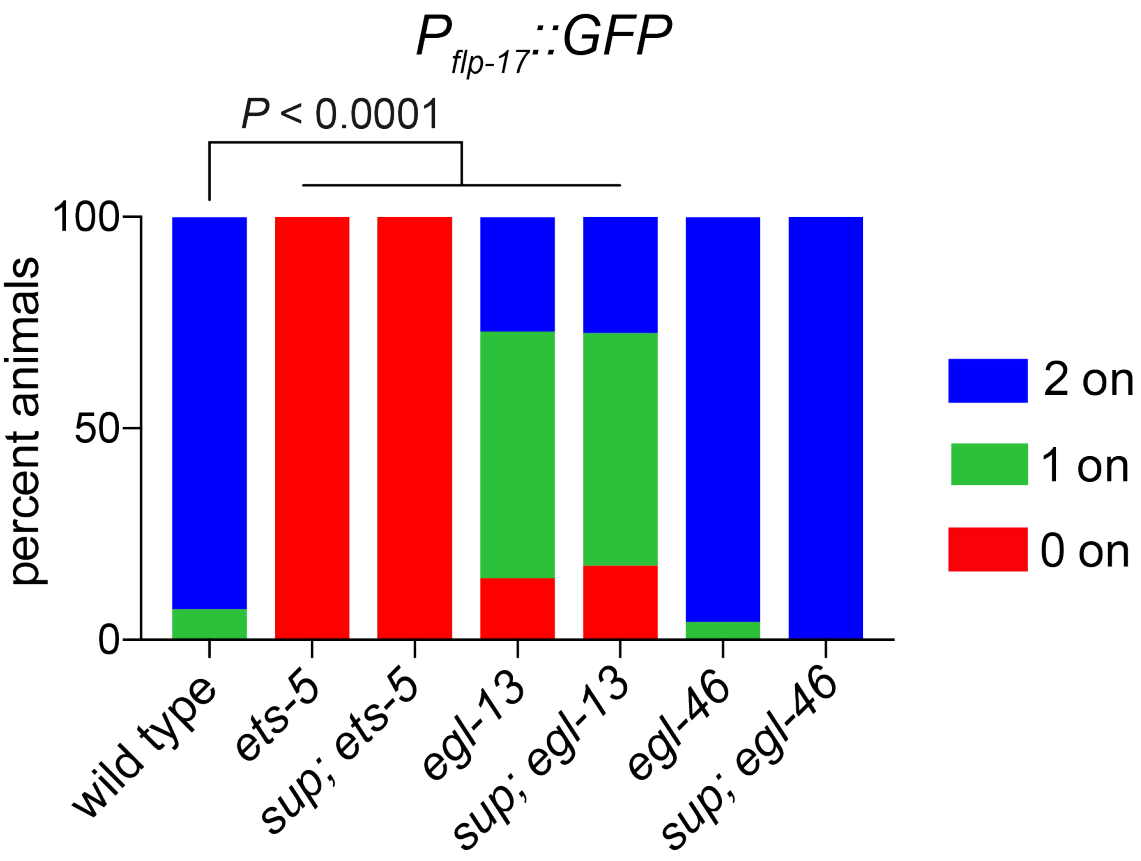

Figure S5: Suppressor mutations do not restore gene expression to mutants for transcription factors that promote a BAG fate.

Penetrance of P_{flp-17}*::GFP* expression in the wild-type, *ets-5(tm1734)*, *sup(e169); ets-5(tm1734)*, *egl-13(ku194)*, *sup(e169); egl-13(ku194)*, *egl-46(n1075)*, and *sup(e169); egl-46(n1075)* mutant animals. While *ets-5* and *egl-13* mutants are significantly defective for *flp-17* expression, the suppressor mutation does not modify their gene expression defects. N ≥ 30 animals/genotype. $P < 0.0001$, chi-square test.

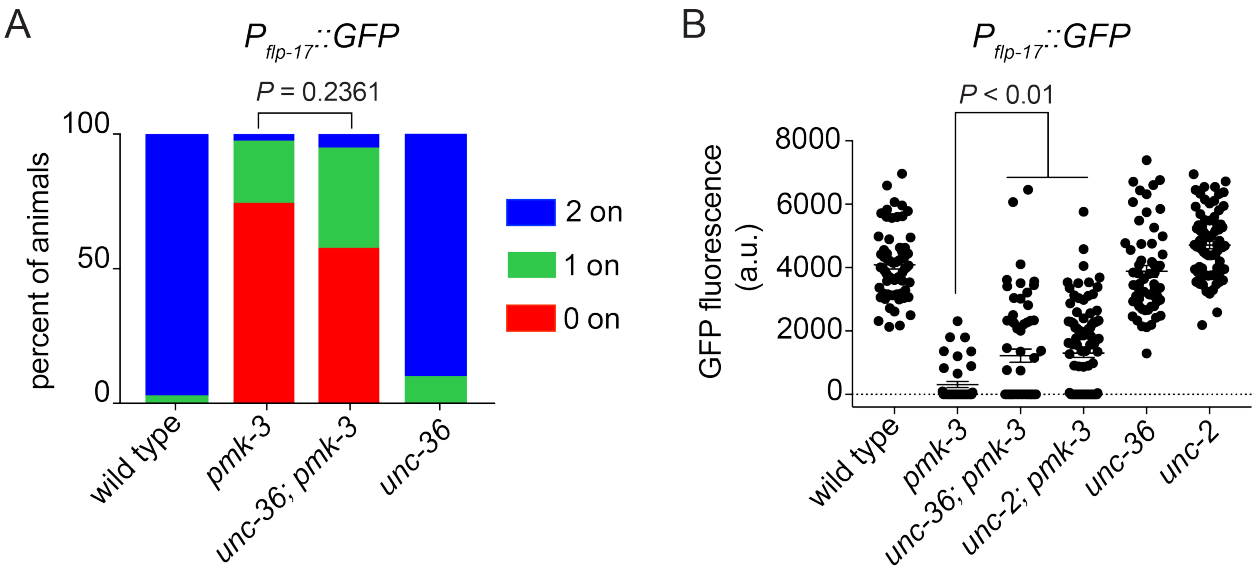

Figure S6: Mutations in NPQ-type Voltage-Gated Calcium Channel subunits restore *flp-17* expression to *pmk-3* mutant BAG neurons.

A. Penetrance of P_{flp-17}*::GFP* expression in the wild-type, *pmk-3(ok169)*, *unc-36(e251); pmk-3(ok169)*, and *unc-36(e251)* mutant animals. N ≥ 30 animals/genotype. *P* = 0.2361, chi-square test.

B. Levels of P_{flp-17}*::GFP* expression in the wild-type, *pmk-3(ok169)*, *unc-36(e251); pmk-3(ok169)*, *pmk-3(ok169); unc-2(e55)*, *unc-36(e251)*, and *unc-2(e55)* mutant animals. N ≥ 30 animals/genotype. *P* = 0.0028 for *pmk-3* vs *unc-36; pmk-3* and *P* = 0.0003 for *pmk-3* vs *pmk-3; unc-2*, ordinary one-way ANOVA followed by Tukey's multiple comparison test. (a.u.) arbitrary units. Error bars represent SEM.

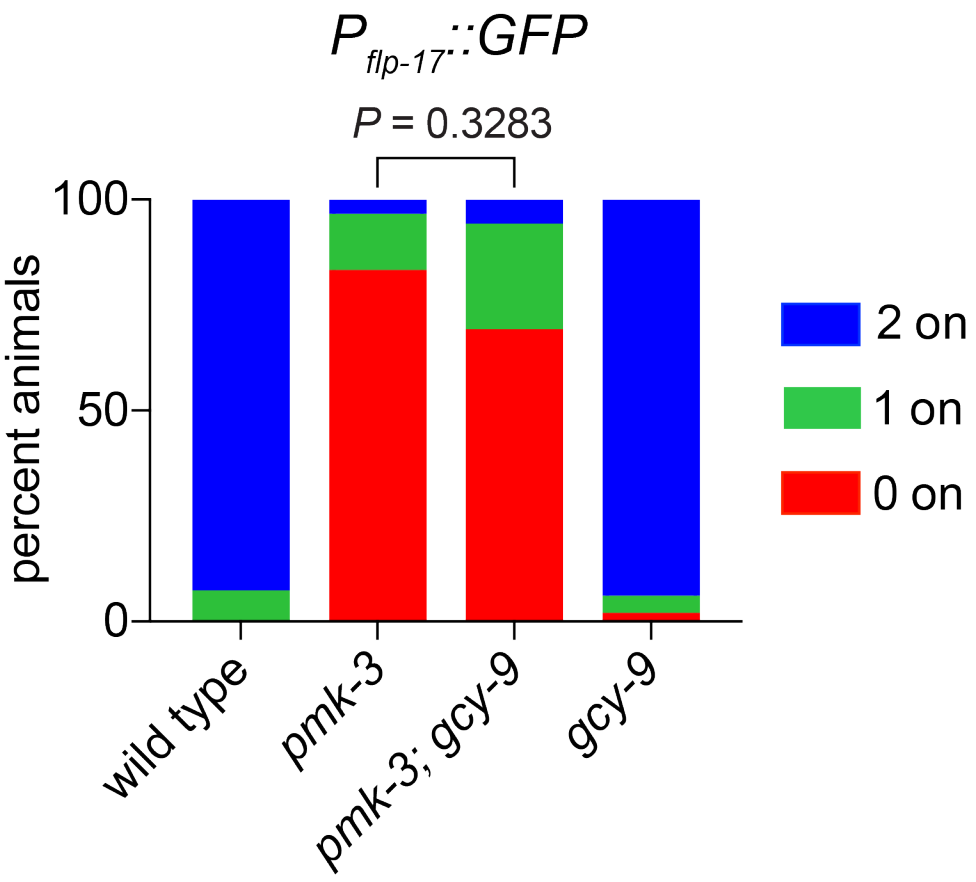

Figure S7: Disrupting CO_2 sensation in *pmk-3* mutant animals does not restore *flp-17* expression to their BAG cells.

The penetrance of P_{flp-17}*::GFP* expression in the wild-type, *pmk-3(ok169)*, *pmk-3(ok169); gcy-9(tm2816)*, and *gcy-9(tm2816)* mutant animals. N > 25 animals/genotype. *P* = 0.3283, chi-square test.

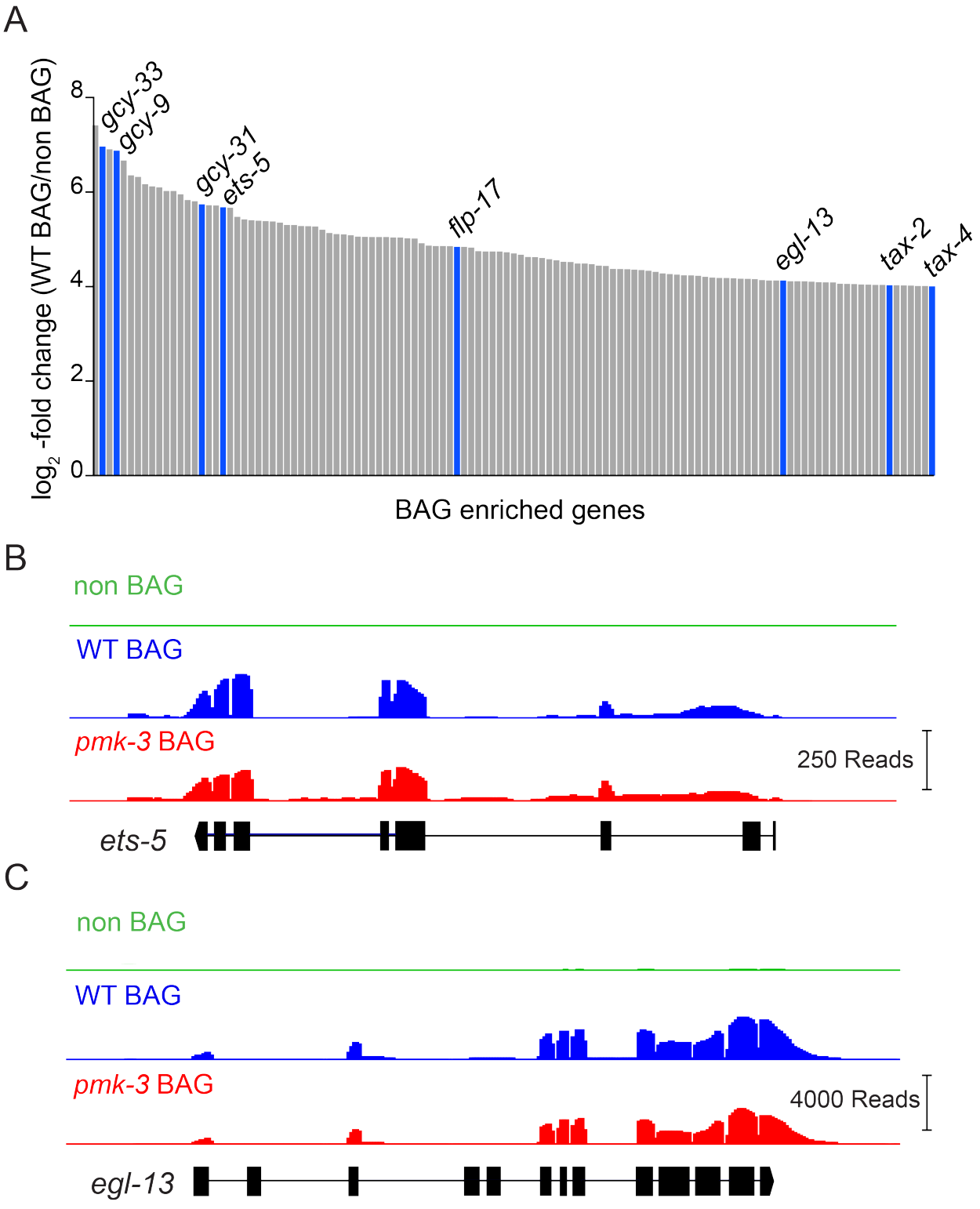

Figure S8: *pmk-3* mutation does not affect expression of the terminal selectors of the BAG cell fate. (legend continued on next page)

A. Fold changes of gene expression for the 119 BAG-enriched transcripts identified with RNA-Seq (log2fold change of expression in wild-type BAG cells versus non-BAG cells > 4). Blue indicates genes already known to be BAG-enriched. (WT) wild-type.

B-C. Read coverage histograms for transcription factors *ets-5* and *egl-13,* which maintain the BAG cell-fate and are the canonical terminal selectors of the BAG neuron.

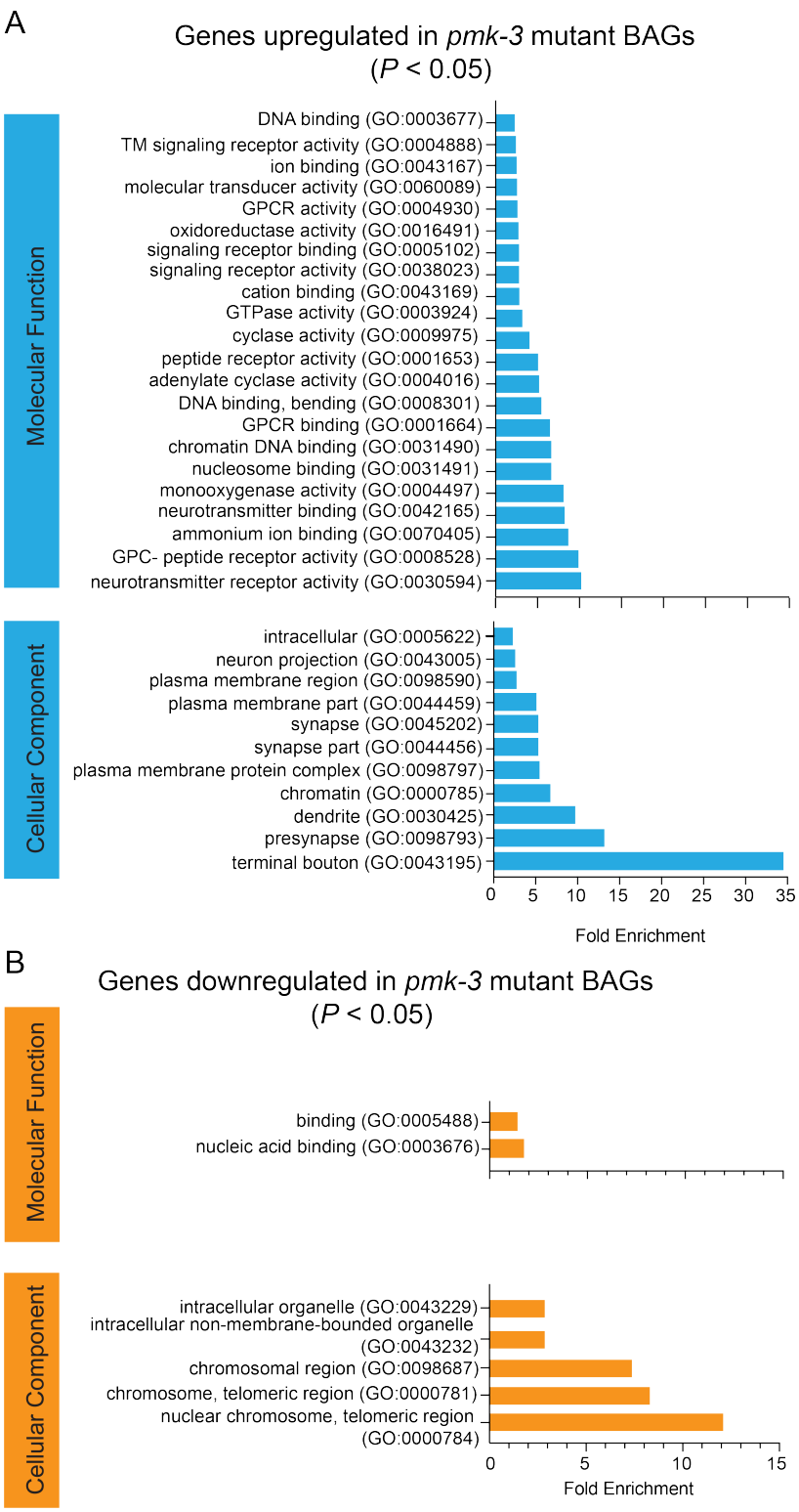

Figure S9: Overrepresented GO terms in genes significantly up-regulated and down-regulated in *pmk-3* mutant BAG cells. (legend continued on next page)

A. Molecular function and cellular component classification terms significantly over-represented ($P < 0.05$) amongst the subset of genes up-regulated in *pmk-3* mutant BAG cells (see Materials and Methods).

B. Molecular function and cellular component GO terms significantly enriched ($P < 0.05$) amongst the set of genes down-regulated in *pmk-3* mutant BAG cells. We note that there wasn't any biological process GO terms that were significantly enriched amongst the genes down-regulated in *pmk-3* mutant BAG cells.

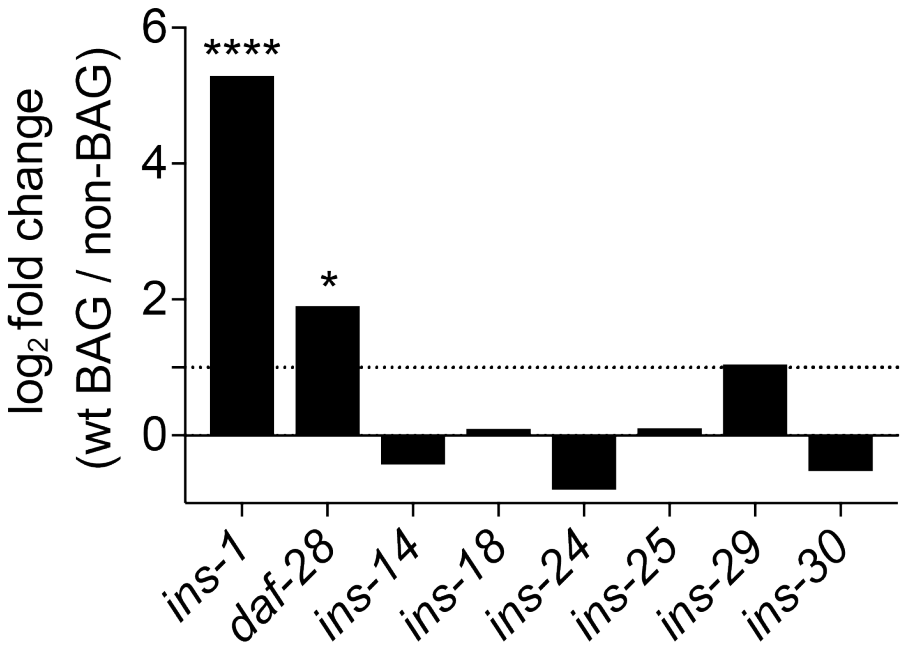

Figure S10: The insulin like peptides (ILPs), *ins-1* and *daf-28*, are enriched in wild-type BAG cells.

Fold changes of gene expression in wild-type BAG cells versus non-BAG cells for *ins*-1 and the ILPs that are enriched in *pmk-3* mutant BAG cells. (*) $P < 0.05$, (****) $P < 0.0001$. *P* values were FDR corrected using DeSeq2 (Love et al., 2014).

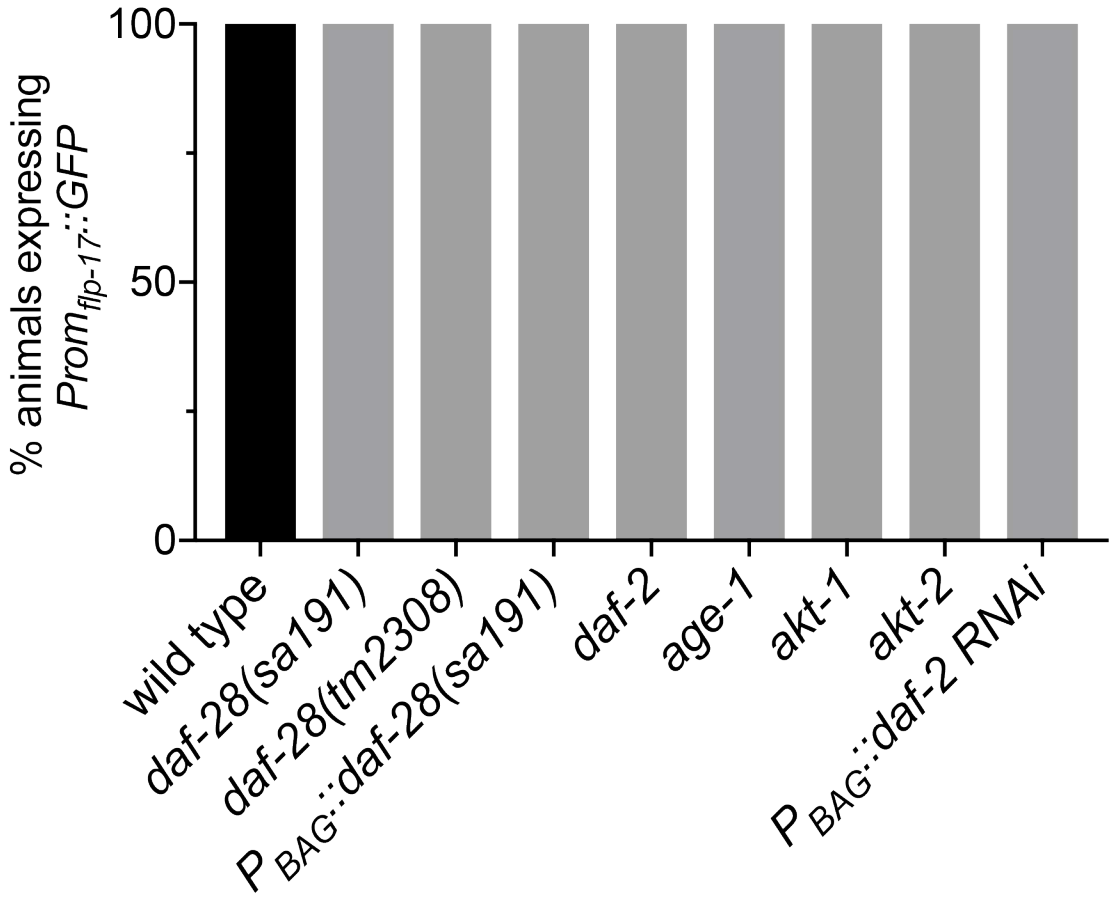

Figure S11: Loss of autocrine insulin signaling does not affect *flp-17* expression in a wild-type background.

Percent animals expressing $P_{flp\text{-}17}$*::GFP* in the wild type, *daf-28(sa191)*, *daf-28(tm2308)*, *daf-2(e1370)*, *age-1(hx546)*, *akt-1(ok525)*, *akt-2(ok393)* mutant animals. Disrupting insulin production in wild-type BAG cells by over-expressing *daf-28(sa191),* P_{BAG}*::daf-28(sa191)*, and BAG cell-specific knockdown of *daf-2* using RNAi, P_{BAG}*::daf-2 RNAi*, also does not affect $P_{flp\text{-}17}$*::GFP* expression. N ≥ 38 animals/genotype.

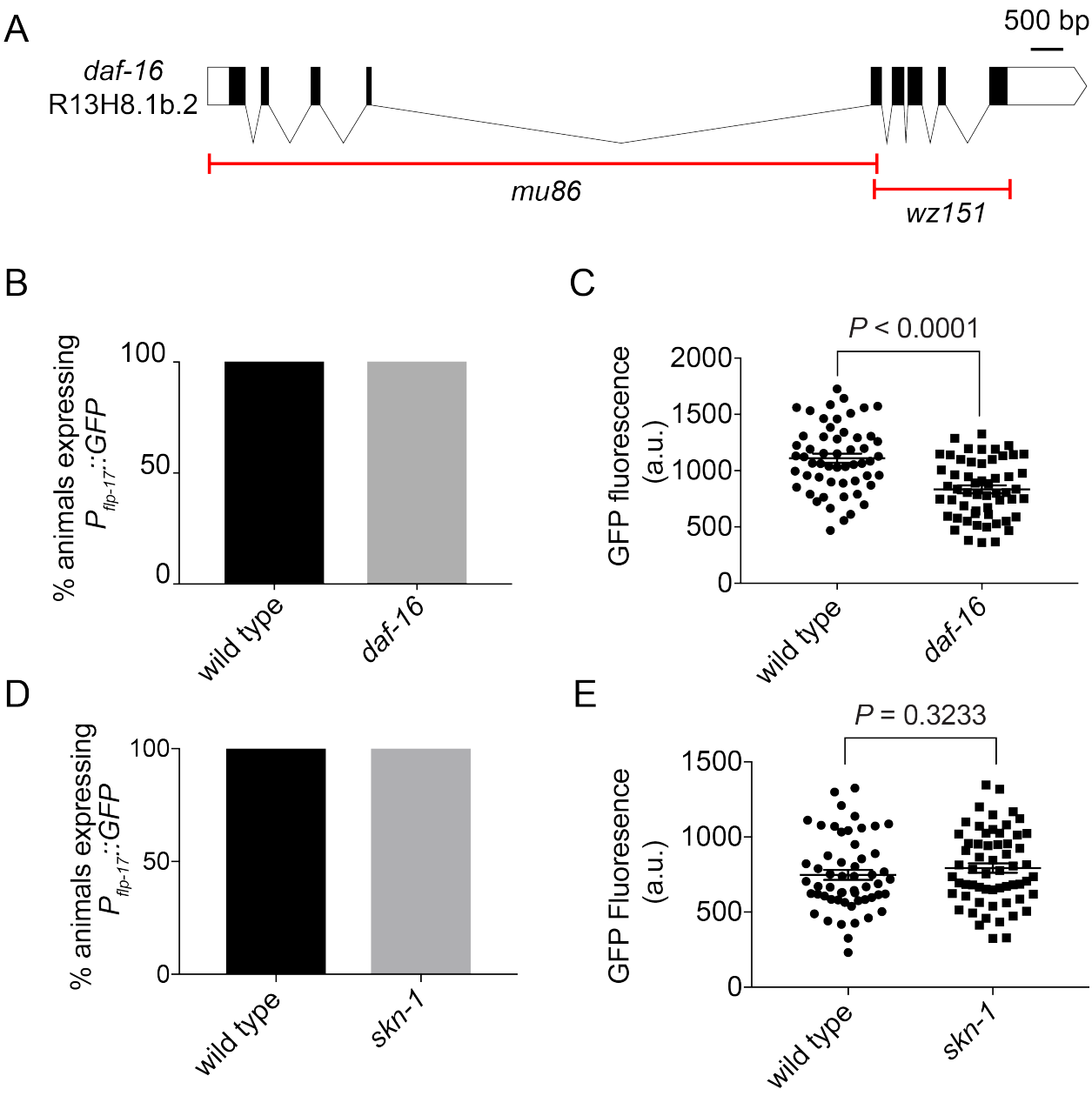

Figure S12: Loss of DAF-16 reduces levels of *flp-17* expression, while loss of SKN-1 has no effect.

A. Structure of the *daf-16* genetic locus showing the canonical null allele, *mu86*, and the *wz151* 2065 base pair deletion allele generated using CRISPR/Cas9 mutagenesis (see Materials and Methods).

(legend continued on next page)

B. Percent wild-type and *daf-16(wz151)* mutant animals expressing P_{flp-17}*::GFP*. N = 28 animals/genotype.

C. Levels of P_{flp-17}*::GFP* fluorescence in the wild-type and *daf-16(wz151)* mutant animals. N = 28 animals/genotype. $P < 0.0001$, unpaired t-test. (a.u.) arbitrary units.

D. Percent wild-type and *skn-1(zu67)* mutant animals expressing P_{flp-17}*::GFP*. Because *skn-1(zu67)* is maternal effect lethal, *skn-1(zu67)* homozygous mutants were picked from heterozygous mothers carrying the *mIs11[myo-2::GFP]* balancer chromosome for analysis. N = 30 animals/genotype.

E. Levels of P_{flp-17}*::GFP* fluorescence in the wild-type and *skn-1(zu67)* mutant animals. N ≥ 28 animals/genotype. $P = 0.3233$, unpaired t-test. (a.u.) arbitrary units.

Error bars represent mean ± SEM.

Table S1: Strains used in this study

Identifier	Genotype	Associated Figure
NY2064	*ynIs64[P_{flp-17}::GFP]; him-5(e1490)*	1A, 2C, 2F, 2G, 3A, 3B, S5, S6, S7, S11, S12
FQ464	*ynIs64[P_{flp-17}::GFP]; pmk-3(wz31)*	1A, 2A, 2C, 2F, S3
N2	wild type	1B, 7A-C
FQ551	*ynIs64[P_{flp-17}::GFP]; pmk-3(ok169)*	1B, 2G, 3A, 3B, 3D, 5B, 5C, 5D, 6A, 6B, 7A-C, S6, S7
MT15933	*flp-17(n4894)*	1B
MT14665	*egl-6(n4536)*	1B
FQ243	*wzIs82[P_{gcy-9}::YC3.60]*	1C, 1D, S1
FQ1779	*wzIs82[P_{gcy-9}::YC3.60]; pmk-3(ok169)*	1C, 1D, S1
FQ2070	*wzIs168[P_{gcy-9}::nlg-1::GFP_{1-10} + P_{odr-2b}::nlg-1::GFP_{11} + P_{gcy-9}::dsRed + $P_{unc-122}$::mCherry]*	1E, 1F, S2
FQ2098	*pmk-3(ok169); wzIs168[P_{gcy-9}::nlg-1::GFP_{1-10} + P_{odr-2b}::nlg-1::GFP_{11} + P_{gcy-9}::dsRed + $P_{unc-122}$::mCherry]*	1E, 1F, S2
FQ841	*ynIs64[P_{flp-17}::GFP]; pmk-3(wz31) unc-31(wz75)*	2B, 2C, S3
FQ1125	*ynIs64[P_{flp-17}::GFP]; unc-31(e169)*	2C, S3
FQ875	*ynIs64[P_{flp-17}::GFP]; pmk-3(wz31) unc-31(wz76)*	2D
FQ1245	*ynIs64[P_{flp-17}::GFP]; pmk-3(wz31) unc-31(wz127)*	2D
FQ1224	*ynIs64[P_{flp-17}::GFP]; pmk-3(wz31) unc-31(wz112) unc-31(wz130)*	2D
FQ873	*ynIs64[P_{flp-17}::GFP]; pmk-3(ok169); him-5(e1490)*	2F
FQ1204	*ynIs64[P_{flp-17}::GFP]; unc-64(e246); pmk-3(wz31)*	2F
FQ1212	*ynIs64[P_{flp-17}::GFP]; unc-64(e246)*	2F
FQ1302	*ynIs64[P_{flp-17}::GFP] unc-13(e51); pmk-3(ok169)*	2F

FQ1268	*ynIs64[P_{flp-17}::GFP] unc-13(e51)*	2F
FQ1301	*ynIs64[P_{flp-17}::GFP]; pmk-3(ok169); unc-18(e81)*	2F
FQ1250	*ynIs64[P_{flp-17}::GFP]; unc-18(e81)*	2F
FQ1244	*ynIs64[P_{flp-17}::GFP]; pmk-3(ok169); unc-2(e55)*	2G
FQ1219	*ynIs64[P_{flp-17}::GFP]; unc-2(e55)*	2G
FQ1308	*ynIs64[P_{flp-17}::GFP]; pmk-3(ok169) egl-19(n582)*	2G
FQ1307	*ynIs64[P_{flp-17}::GFP]; egl-19(n582)*	2G
FQ1637	*ynIs64[P_{flp-17}::GFP]; pmk-3(ok169); wzEx289[P_{gcy-9}::unc-31_sense+P_{gcy-9}::unc-31_antisense + $P_{unc-122}$::mCherry]*	3B
FQ1638	*ynIs64[P_{flp-17}::GFP]; wzEx289[P_{gcy-9}::unc-31_sense + P_{gcy-9}::unc-31_antisense + $P_{unc-122}$::mCherry]*	3B
FQ1612	*ynIs64[P_{flp-17}::GFP]; pmk-3(ok169); wzEx457[P_{rab-3}::unc-31_sense + P_{rab-3}::unc-31_antisense + $P_{unc-122}$::mCherry]*	3B
FQ1657	*ynIs64[P_{flp-17}::GFP]; wzEx457[P_{rab-3}::unc-31_sense + P_{rab-3}::unc-31_antisense + $P_{unc-122}$::mCherry]*	3B
FQ1443	*ynIs64[P_{flp-17}::GFP]*	3B
FQ1665	*ynIs64[P_{flp-17}::GFP]; pmk-3(ok169); wzEx467[P_{gcy-9}::irk-1 + $P_{unc-122}$::mCherry]*	3A
FQ1710	*ynIs64[P_{flp-17}::GFP]; wzEx467[P_{gcy-9}::irk-1 + $P_{unc-122}$::mCherry]*	3A
FQ1414	*ynIs64[P_{flp-17}::GFP]; pmk-3(ok169); wzEx395[P_{rab-3}::irk-1 + $P_{unc-122}$::mCherry]*	3A

FQ1438	*ynIs64[P_{flp-17}::GFP]; wzEx395[P_{rab-3}::irk-1 + $P_{unc-122}$::mCherry]*	3A
FQ1601	*ynIs64[P_{flp-17}::GFP]; pmk-3(ok169); wzEx448[$P_{hsp16.4}$::irk-1 + $P_{unc-122}$::mCherry]*	3D
FQ424	*wzIs113[P_{gcy-9}::GFP]*	4A-I
FQ705	*wzIs113[P_{gcy-9}::GFP]; pmk-3(wz31)*	4A-I
FQ1767	*ynIs64[P_{flp-17}::GFP]; pmk-3(ok169); daf-28(tm2308)*	5C
FQ1641	*ynIs64[P_{flp-17}::GFP]; pmk-3(ok169); daf-28(sa191)*	5B, 7A
FQ1913	*ynIs64[P_{flp-17}::GFP]; pmk-3(ok169); wzEx519[P_{gcy-9}::daf-28(sa191) + $P_{unc-122}$::mCherry]*	5B, 7B
FQ1409	*ynIs64[P_{flp-17}::GFP]; daf-2(e1370); pmk-3(ok169)*	5D
FQ1632	*ynIs64[P_{flp-17}::GFP]; age-1(hx546); pmk-3(ok169)*	5D, 6B
FQ1872	*ynis64[P_{flp-17}::GFP]; pmk-3(ok169); akt-1(ok525)*	5D
FQ1876	*ynIs64[P_{flp-17}::GFP]; pmk-3(ok169); akt-2(ok393)*	5D
FQ2056	*wzEx542[P_{gcy-9}::daf-16::GFP + P_{gcy-9}::dsRed + $P_{unc-122}$::mCherry]*	5E, 5F
FQ2094	*daf-2(e1370); wzEx542[P_{gcy-9}::daf-16::GFP + P_{gcy-9}::dsRed + $P_{unc-122}$::mCherry]*	5E, 5G
FQ2074	*pmk-3(ok169); wzEx542[P_{gcy-9}::daf-16::GFP + P_{gcy-9}::dsRed + $P_{unc-122}$::mCherry]*	5F
FQ2127	*daf-2(e1370); pmk-3(ok169); wzEx542[P_{gcy-9}::daf-16::GFP + P_{gcy-9}::dsRed + $P_{unc-122}$::mCherry]*	5G

FQ1481	*ynis64[P_{flp-17}::GFP]; pmk-3(ok169); wzEx408[P_{flp-17}::daf-2_sense + P_{flp-17}::daf-2_antisense + $P_{unc-122}$::mCherry]*	5D, 6A, 7C
FQ1778	*ynIs64[P_{flp-17}::GFP] daf-16(wz151); pmk-3(ok169)*	6A
FQ1777	*ynIs64[P_{flp-17}::GFP] daf-16(wz151); pmk-3(ok169); wzEx408[P_{flp-17}::daf-2_sense + P_{flp-17}::daf-2_antisense + $P_{unc-122}$::mCherry]*	6A
FQ2289	*ynIs64[P_{flp-17}::GFP]; pmk-3(ok169); wzEx574[P_{gcy-9}::skn-1_sense + P_{gcy-9}::skn-1_antisense+$P_{unc-122}$::mCherry]*	6B
FQ2253	*ynIs64[P_{flp-17}::GFP]; age-1(hx546); pmk-3(ok169); wzEx574[P_{gcy-9}::skn-1_sense + P_{gcy-9}::skn-1_antisense+$P_{unc-122}$::mCherry]*	6B
FQ1740	*ynIs64[P_{flp-17}::GFP]; daf-28(sa191)*	7A, S11
FQ1531	*ynis64[P_{flp-17}::GFP]; wzEx408[P_{flp-17}::daf-2_sense + P_{flp-17}::daf-2_antisense + $P_{unc-122}$::mCherry]*	7C, S11
Strains in Supplemental Figures		
MT17370	*nIs242[P_{gcy-33}::GFP]; lin-15AB(n765)*	S4
FQ932	*nIs242[P_{gcy-33}::GFP]; pmk-3(wz31)*	S4
FQ1099	*nIs242[P_{gcy-33}::GFP]; pmk-3(wz31) unc-31(wz75)*	S4
FQ1131	*nIs242[P_{gcy-33}::GFP]; unc-31(e169)*	S4
FQ223	*ynis64[P_{flp-17}::GFP]; ets-5(tm1734)*	S5
FQ2284	*ynis64[P_{flp-17}::GFP]; unc-31(e169); ets-5(tm1734)*	S5
FQ2301	*ynis64[P_{flp-17}::GFP]; egl-13(ku194)*	S5
FQ2300	*ynis64[P_{flp-17}::GFP]; unc-31(e169); egl-13(ku194)*	S5
FQ2303	*ynis64[P_{flp-17}::GFP]; egl-46(n1075)*	S5
FQ2302	*ynis64[P_{flp-17}::GFP]; unc-31(e169); egl-46(n1075)*	S5
FQ1243	*ynIs64[P_{flp-17}::GFP]; unc-36(e251); pmk-3(ok169)*	S6

FQ1220	*ynIs64[P_{flp-17}::GFP]; unc-36(e251)*	S6
FQ1303	*ynIs64[P_{flp-17}::GFP]*; *pmk-3(ok169)*; *gcy-9(tm2816)*	S7
FQ1289	*ynIs64[P_{flp-17}::GFP]*; *gcy-9(tm2816)*	S7
FQ1768	*ynIs64[P_{flp-17}::GFP]*; *daf-28(tm2308)*	S11
FQ1934	*ynIs64[P_{flp-17}::GFP]*; *wzEx519[P_{gcy-9}::daf-28(sa191) + $P_{unc-122}$::mCherry]*	S11
FQ1381	*ynIs64[P_{flp-17}::GFP]*; *daf-2(1370)*	S11
FQ1634	*ynIs64[P_{flp-17}::GFP]*; *age-1(hx546)*	S11
FQ1874	*ynIs64[P_{flp-17}::GFP]*; *akt-1(ok525)*	S11
FQ1877	*ynIs64[P_{flp-17}::GFP]*; *akt-2(ok393)*	S11
FQ1758	*ynIs64[P_{flp-17}::GFP] daf-16(wz151)*	S12A,B, C
FQ1838	*ynIs64[P_{flp-17}::GFP; mIs11[myo-2::GFP]/skn-1(zu67)*	S12D, E
FQ1934	*ynIs64[Pflp-17::GFP]*; *wzEx519[P_{gcy-9}::daf-28(sa191) + $P_{unc-122}$::mCherry]*	S12

Table S2: Plasmids used in this study

Constructed Plasmid Name	Description	Injected Concentration
pNR634	P_{gcy-9}*::nlg-1::GFP*$_{1-10}$	10 - 20 ng ul^{-1}
pNR631	P_{odr-2b}*::nlg-1::GFP*$_{11}$	10 - 20 ng ul^{-1}
pLBH10	P_{gcy-9}*::unc-31_sense*	100 ng ul^{-1}
pLBH9	P_{gcy-9}*::unc-31_antisense*	100 ng ul^{-1}
pLBH50	P_{rab-3}*::unc-31_sense*	100 ng ul^{-1}
pLBH51	P_{rab-3}*::unc-31_antisense*	100 ng ul^{-1}
pLBH21	P_{gcy-9}*::irk-1*	100 ng ul^{-1}
pLBH26	P_{rab-3}*::irk-1*	100 ng ul^{-1}
pLBH49	$P_{hsp-16.4}$*::irk-1*	100 ng ul^{-1}
pNR394	P_{gcy-9}*::dsRed*	30 ng ul^{-1}
pLBH57	P_{gcy-9}*::daf-28(sa191)*	25 ng ul^{-1}
pLBH43	P_{flp-17}*::daf-2_sense*	100 ng ul^{-1}
pLBH44	P_{flp-17}*::daf-2_antisense*	100 ng ul^{-1}
pLBH56	P_{gcy-9}*::daf-16::GFP*	30 ng ul^{-1}
pLBH61	P_{gcy-9}*::skn-1_sense*	100 ng ul^{-1}
pLBH62	P_{gcy-9}*::skn-1_antisense*	100 ng ul^{-1}
Co-injection marker	$P_{unc-122}$*::mCherry*	30 - 100 ng ul^{-1}